

## Trapping of Single Magnetic Beads in a Micro Flow

H. Chen<sup>1,2</sup> and Y. Zhu<sup>1,2,3</sup>

<sup>1</sup> CSIRO Manufacturing, Private Bag 10, Clayton 3168, Australia

<sup>2</sup> Harbin Institute of Technology (Shenzhen), Shenzhen, 518055, China

<sup>3</sup> School of Science, RMIT University, Melbourne, VIC 3001, Australia

### Abstract

Superparamagnetic microbeads have been widely applied in immunoassay and separation of target analytes from biological samples in microfluidics, since their large surface-area-to-volume ratio is able to increase the detection sensitivity or separation efficiency and they can be easily manipulated using an external magnetic field. This paper reports both experimental and numerical studies of the single bead trapping on a permalloy microarray in the presence of a micro flow and an external magnetic field. The permalloy microarray consists of microstructures measuring  $4\ \mu\text{m}$  (width)  $\times$   $20\ \mu\text{m}$  (length)  $\times$   $0.3\ \mu\text{m}$  (thickness). The width of the magnetic trap formed between two adjacent microstructures is  $3\ \mu\text{m}$ . After microbeads ( $5\text{-}5.9\ \mu\text{m}$  in diameter) were injected onto the permalloy microarray in a microchannel, single beads were captured in the traps. The retention of beads at a given magnetic field and various fluid flow rates was experimentally studied. A single-bead model is developed to numerically study the magnetic force and fluid-induced drag on the bead. The magnetic force is studied to determine the position of the beads with maximal magnetic force. Finally, a mechanical equilibrium model is introduced to explain the single bead trapping mechanism. This paper provides a guide for the design of microstructures trapping magnetic microbeads in microfluidic channels with fluid flow.

### Introduction

Superparamagnetic microbeads have been widely applied in microfluidics for immunoassay and separation of target analytes from biological samples [1, 17], since i) their large surface-area-to-volume ratio is able to increase the detection sensitivity or separation efficiency, ii) they can be easily manipulated by external magnetic field and iii) colour-coded beads enable high-throughput multiplexed detection [10]. Trapping of microbeads in the microfluidic channel is the most important process for the applications mentioned above, because it allows rapid and efficient washing and separation of the samples. The magnetic field outside the microchannel [1, 8], microstructures integrated in the microchannel [6], micro electromagnets [13], and disk-shaped micromagnets [9, 16] have been employed to trap microbeads. However, these methods are able to neither control the number of trapped beads nor capture single beads. Although, micromagnets [9] are of the potential to capture single beads in theory, they block the light path for fluorescent imaging of the beads using an inverted microscope. Therefore, in order to apply microfluidics in immunoassay, it is critical to develop a reliable single bead trapping technique with the ability of controlling bead-surface-area-to-sample-volume ratio and fluorescent imaging.

Chen et al. recently developed the high-throughput and reliable trapping technique of single beads using a permalloy microarray in the presence of an external magnetic field. This tapping

mechanism modified from previous work [2] has proved to be simple and reliable. In addition, it has been successfully integrated with acoustic micromixing for rapid multiplexed immunoassay.

Analysis of the magnetic behaviour, in particular, the magnetic force of the trapped single bead in microfluidics is critical for their successful implementation. Analytical solution of a magnetic field around a sphere within a magnetic field is well known [12]. In addition, the magnetic force on the bead in the microchannel with external magnetic field [7, 15] has been reported. However, it is hard to analytically study the magnetic force on a bead which is within the magnetic field generated by external magnets but locally focused by magnetic microstructures. To our best knowledge, there is neither an analytical solution nor literature describing the magnetic force subjected by the single bead trapped between two poles of the microstructures/magnets. Understanding the mechanism of single bead trapping in such magnetic traps in the presence of micro flow is able to guide the design of microfluidic devices for single-bead based applications.

This paper aims to both experimentally and numerically study the trapping of single beads in the permalloy microarray with the external magnetic field and the micro flow. The bead displacement at various flow rates was experimentally determined. The fluid-induced drag on the bead was numerically studied when flow rates varied. The magnetic force on the bead was modelled when the bead was displaced away from the magnetic trap. Finally, a mechanical model was proposed to understand the trapping mechanism.

### Materials and Methods

#### Device Fabrication

The device consists of a PDMS layer with a straight microchannel and a permalloy microarray coated on a glass slide. The microchannel is  $100\ \mu\text{m}$  wide and  $40\ \mu\text{m}$  deep. The PDMS layer was fabricated by standard soft lithography [4, 5]. The permalloy microarray was sputtered on a glass slide using physical vapour deposition. The microarray consists of repetitive permalloy microstructures (see Figure 1), which are  $4\ \mu\text{m}$  (width)  $\times$   $20\ \mu\text{m}$  (length)  $\times$   $0.3\ \mu\text{m}$  (thickness). They are spaced at  $3\ \mu\text{m}$  and  $20\ \mu\text{m}$  in Y and X directions, respectively.

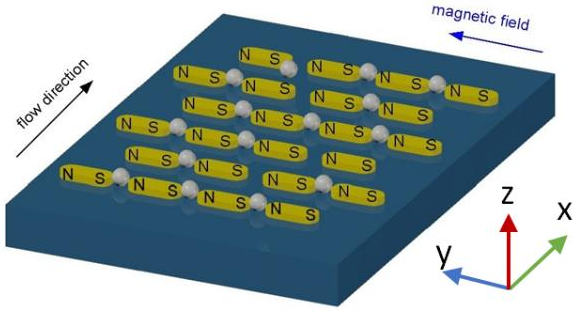


Figure 1. The schematic drawing of single beads trapped by the permalloy microarray on a glass slide. After the introduction of an external magnetic field, permalloy microstructures are magnetized as individual magnets. Single magnetic beads are captured in the gap of two adjacent microstructures.

### Bead Displacement Study

The device was mounted on the stage of an inverted microscope. Two permanent magnets were placed on both sides of the microchannel. Then the solution of SPHERO™ carboxyl magnetic microbeads (5-5.9  $\mu\text{m}$  in diameter) with the concentration of 1 million beads per ml was manually injected into the microchannel. After beads were captured by the permalloy microarray, a phosphate buffer solution with 0.05% Triton X-100 (PBST) was injected into the channel at the flow rate of 1 nL/sec to flush away excessive beads from the microarray. Then PBST was injected into the microchannel at flow rates from 2 nL/sec to 5  $\mu\text{L}/\text{sec}$ . Finally, the beads were imaged to record their positions with and without the flow of PBST.

### Numerical Study

The magnetic force and fluid-induced drag on the trapped beads were numerically studied using COMSOL Multiphysics software to understand the trapping mechanism of single beads in the micro flow and the locally focused magnetic field.

A single bead model with two permalloy microstructures was employed for the magnetic force study. The magnetic trap was 3  $\mu\text{m}$  wide. The permalloy microstructure was 300 nm thick. The diameter of the bead was 5.6  $\mu\text{m}$ . The position of the bead was varied from the trap centre ( $x=0$ ) to 4  $\mu\text{m}$  ( $x=4 \mu\text{m}$ ) away in the downstream to simulate the potential displacement of the single bead as a result of the micro flow. The external magnetic field strength was 0.98 G. The magnetic permeability of the permalloy microarray and the bead is 174 and 11.3, respectively. The bead in the experiment was an iron oxide sphere within a polystyrene shell, but the size of the iron oxide was unavailable. Therefore, the whole bead was assumed to be an iron oxide sphere in the simulation. The mesh size was optimised in order to acquire mesh-independent result.

The fluid-induced drag on the single bead in a micro flow was simulated using a simplified single-bead model. Since the permalloy microarray is 300 nm thick, which is less than 1/100 of the channel height, it is a reasonable assumption that the permalloy microarray has no influence on the flow around the bead. Therefore, the microarray was not considered in the modelling of the fluid flow. The channel in the model was 40  $\mu\text{m}$  high and 40  $\mu\text{m}$  wide. The side walls were set as symmetric boundaries, which suggests that the width of the channel has no impact on the drag force of the bead. A fully developed flow with a parabolic flow profile was modelled. The parabolic flow profile ( $V_{in}$ ) at the inlet port is given by:

$$V_{in} = 6 \frac{q}{wh} \left[ -\left(\frac{z}{h}\right)^2 + \frac{z}{h} \right] \quad (1)$$

where  $q$  is the volumetric flow rate,  $w$  and  $h$  are the width and height of the microchannel, respectively,  $z$  is the coordinate in the height direction. The inlet flow rate ( $q$ ) varied from 1 to 15 nL/sec.

In order to validate the accuracy of this model, the drag on a bead fixed in a Couette flow was numerically studied in the same way. The drag from the modelling was then compared to its analytical solution [3].

### Magnetic Field Measurement

A hall-effect Gauss meter was used to measure the magnetic field applied on the microarray. Since two external magnets were approximately two centimetres away from each other and the microarray is only 100  $\mu\text{m}$  wide in the direction (Y direction in Figure 1) of the magnetic field, it is a reasonable assumption that the magnetic field gradient in the permalloy microarray is negligible. The magnetic field strength of this study was measured as 0.98 G.

### Image and Data Analysis

The images obtained in the bead displacement study were analysed using Image J software [14] to determine the displacement of the single beads after the injection of the PBST. Error bars represent the standard error of mean. Both linear and non-linear regression analyses of the data were performed using Matlab.

## Results and Discussion

### Bead Displacement Study

Displacement of beads along the flow direction (X) was studied to understand the behavior of single beads in the magnetic traps, when flow rates varied from 1 nL/sec to 5 nL/sec. In the presence of the external magnetic field, permalloy microstructures are magnetized as individual magnets. As a result, a magnetic trap forms between the opposite poles of two adjacent micromagnets (see Figure 1). After loading of the bead solution, single magnetic beads are captured by the traps in the permalloy array. When PBST was injected into the channel, the fluid flow was capable of displacing trapped bead away from the trap center. However, the bead is able to be retained in the vicinity of the trap center, before the flow rate reaches its critical value at which the bead was flushed away from the trap by the microflow.

Figure 2 A and B show the positions of single beads before and after the injection of PBST at 4 nL/sec. The displacement of trapped beads was obvious. The bead displacement when PBST was injected into the microchannel at the flow rate of 2-5 nL/sec was shown in Figure 2C. When the flow rate was 2 nL/sec, the single beads moved 0.54  $\mu\text{m}$  downstream. As the flow rate became higher, the displacement raised. When the flow rate increased to 5 nL/sec, the bead was displaced for 0.98  $\mu\text{m}$ . At such a big flow rate, a large percentage of single beads were still retained in the magnetic traps.

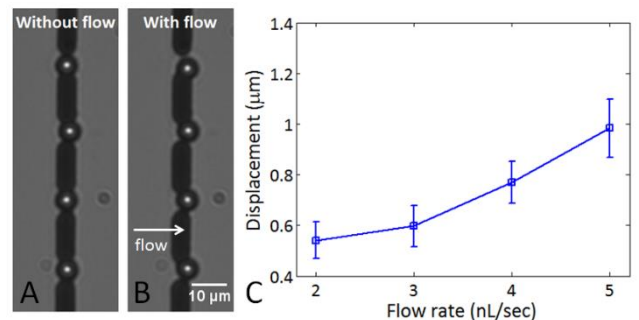


Figure 2. Displacement of single beads in the 3- $\mu\text{m}$  wide traps with the micro flow. Micrograph of beads (A) without and (B) with the flow of PBST at 4 nL/sec. C) The displacement of single beads when PBST was injected at various flow rates.

## Numerical Study

The magnetic force on the single bead when it was displaced for 0-4 microns was numerically studied in order to understand the relationship between the magnetic force and the displacement as well as the critical displacement of the trapped beads. The critical displacement refers to the position of the bead, when it is subject to the maximal magnetic force in  $-X$  direction. The Y component of the magnetic force is one to five orders of magnitude smaller than those in  $-X$  and  $-Z$  directions (see Figure 1 for coordinates), thus it is negligible. This study only discusses the magnetic forces in  $-X$  and  $-Z$  directions. Figure 3 shows the variation of the magnetic force components (in  $-X$  and  $-Z$  directions) when the single bead was flushed 0-4  $\mu\text{m}$  away from the trap centre. As the increase of the displacement from 0 to 4  $\mu\text{m}$ , the magnetic force in  $-Z$  direction dramatically decreased from 238.4 pN to 11.37 pN. While the magnetic force in  $-X$  direction firstly increased from 0 to 52.8 pN when the bead moved 2  $\mu\text{m}$  away from the trap centre and then dropped down to 30.8 pN when the bead was further displaced for 4  $\mu\text{m}$ . The relationship between the X component ( $F_{m1}$ ) of the magnetic force and the bead displacement ( $d$ ) is described by the model below ( $R^2=0.98$ ):

$$F_{m1} = -150.3d^{1.153} + 192.9d \quad (2)$$

The maximal X component of the magnetic force ( $F_{m1Max}$ ) and critical displacement ( $d_c$ ) can be determined by the first order derivative of Equation 2. Therefore, when the bead was 2.013  $\mu\text{m}$  ( $d_c$ ) away from the trap centre, it is subjected to the maximum magnetic force ( $F_{m1Max}$ ) of 51.6 pN in X direction. In addition, from the model it is found that when  $d$  is equal to either 0 or 5.11  $\mu\text{m}$ ,  $F_{m1}$  on the bead becomes zero.

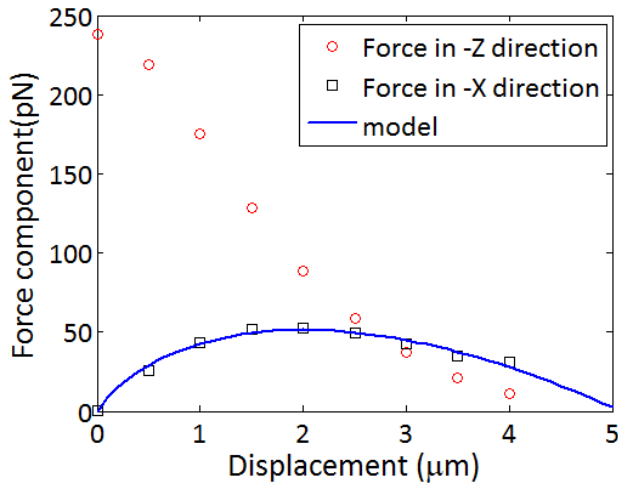


Figure 3. The magnitude of the magnetic force components when the displacement of single beads varied. The relationship between the x component ( $F_{m1}$ ) of the magnetic force and the bead displacement ( $d$ ) is described by ( $R^2 = 0.98$ ):  $F_{m1} = -150.3d^{1.153} + 192.9d$ .

By comparing the trap position of a bead to the critical displacement ( $d_c$ ), one can predict if the flow rate is high enough to flush the single bead away from the magnetic trap. This suggests why the beads were still retained in the magnetic traps, when the beads were displaced for 0.98  $\mu\text{m}$  in the bead displacement experiment.

The analytical solution of the drag on a sphere in Couette flow was applied to validate the accuracy of the modelling. There is only 1.7% difference of the drags between the analytical and the numerical solutions, so the modelling of drag on the bead is proved to be accurate enough. Thus it was employed to analyse the drag on a single bead fixed on the floor of a microfluidic channel with

fully developed flow profile to study the influence of flow on the drag.

The Y and Z components of the drag are negligible compared to the X component. The drag force in X direction ( $D$ ) is linear proportional to the flow rate (see Figure 4). As the increase of the flow rate from 1 to 15 nL/sec, the drag force in X direction raised from 8.6 pN to 131.1 pN. A linear model ( $R^2=0.9995$ ) was employed to fit the data:

$$D = 8.786q \quad (3)$$

where  $q$  is the inlet flow rate (nL/sec). From the model, it is found that the drag on the bead will continue to linearly increase before the bead was flushed away.

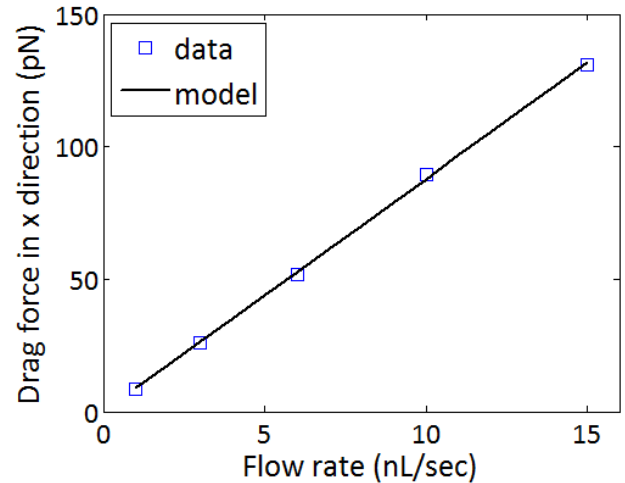


Figure 4. The X component of the fluid-induced drag on the bead in a fully developed micro flow. The relationship between the drag ( $D$ ) and the inlet flow rate ( $q$ ) is described by a linear model ( $R^2=0.9995$ ):  $D = 8.786q$ .

## Mechanical Equilibrium Analysis

When stably retained in the magnetic trap with a fully developed flow, the single bead is subject to forces shown in Figure 5. The forces in Z direction are always in equilibrium, which is described by the following equation:

$$N + F_b + F_{m2} + G = 0 \quad (4)$$

where  $N$  is the normal force from the channel floor,  $F_b$  is the buoyancy force,  $F_{m2}$  is the Z component of the magnetic force, and  $G$  is the gravitational force. Thus, the bead has no motion in z direction.

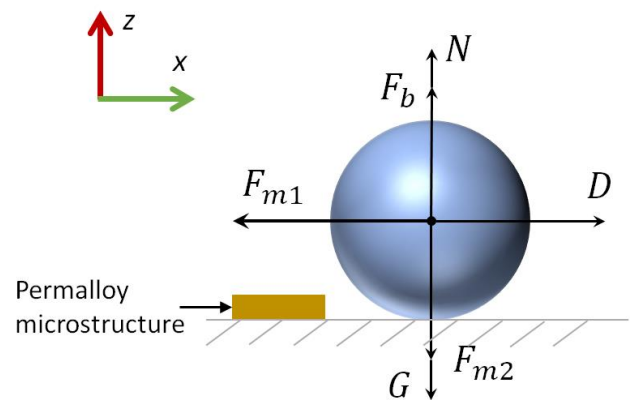


Figure 5. The forces subjected by the single bead captured in the magnetic trap with the micro flow. Flow is in X direction. The bead is displaced downstream of the permalloy microtrap.

The bead is only subjected to two forces in X direction: the X component ( $F_{m1}$ ) of the magnetic force and the fluid-induced drag ( $D$ ). If  $F_{m1} < D$ , the drag will move the bead downward. If  $F_{m1} > D$ , the bead is attracted to the trap by the magnetic force. When  $F_{m1} = D$ , the bead is trapped stably. Therefore, from Equations 2 and 3, the following equation for the mechanical equilibrium is acquired:

$$q = -17.11d^{1.153} + 21.96d \quad (5)$$

The maximal flow rate ( $q_{max}$ ) of 5.87 nL/sec is determined when the displacement reaches its maximum ( $d_c = 2.013 \mu\text{m}$ ). From Equation 5, it is also found that when  $q$  is equal to 2 nL/sec and 5 nL/sec, the displacement ( $d$ ) is equal to 0.25  $\mu\text{m}$  and 1.07  $\mu\text{m}$ , respectively. In the bead displacement experiment, at the flow rate of 2 nL/sec and 5 nL/sec, the mean ( $\pm$  standard deviation) displacement of the beads is 0.54 ( $\pm 0.07$ )  $\mu\text{m}$  and 0.98 ( $\pm 0.114$ )  $\mu\text{m}$ , respectively. So Equation 5 cannot precisely predict the bead displacement by the flow rate. Additionally, in the experiment, when the flow rate was no bigger than 5 nL/sec (in another word,  $q < q_{max}$ ), some beads had already been completely flushed away from the traps. This problem is mostly related to the inaccuracy of the constants in Equation 2 as a result of a) the non-uniformity of the permalloy microstructures, which results in different magnetic forces in distinct traps, b) the inaccuracy of the magnetic force acquired from the simulation due to the assumption that the whole bead is made of iron oxide and c) the error in measurement of the external magnetic field strength. If the above issues are properly solved, the constants in Equation 2 can be modified to allow quantitatively study of the mechanical equilibrium of a single bead captured in the permalloy microarray in the presence of the external magnetic field and the micro flow.

Therefore, the following general equation is proposed to describe the relationship between the flow rate and the displacement ( $d$ ) of the trapped single bead.

$$q = ad^b + cd \quad (6)$$

where  $a$ ,  $b$  and  $c$  are constants related to the magnetic field strength, permalloy microstructure uniformity, magnetic properties of the single bead, and size of the iron core inside the bead.

## Conclusions

This paper reports both experimental and numerical analyses of single bead trapping in a permalloy microarray with liquid flow in a microfluidic channel and an external magnetic field. The displacement of single beads when the flow rate varied was firstly imaged and analysed. Then the magnetic force on a trapped single bead was numerically studied. The critical bead displacement and maximal magnetic force were determined. The drag force was proved to be linearly proportional to the flow rate. Finally, a mechanical equilibrium model was introduced to understand the trapping mechanism of single beads. This paper provides a guide for the designs of microstructures trapping magnetic microbeads in microfluidic channels with fluid flow.

## Acknowledgments

This work was performed in part at the Melbourne Centre for Nanofabrication (MCN) in the Victorian Node of the Australian National Fabrication Facility (ANFF).

## References

- [1] Bronzeau, S. and N. Pamme, *Simultaneous bioassays in a microfluidic channel on plugs of different magnetic particles*. *Analytica Chimica Acta*, 2008. **609**(1): p. 105-112.

- [2] Cao, Q.L., X.T. Han, and L. Li, *Configurations and control of magnetic fields for manipulating magnetic particles in microfluidic applications: magnet systems and manipulation mechanisms*. *Lab on a Chip*, 2014. **14**(15): p. 2762-2777.
- [3] Capretto, L., et al., *Micromixing Within Microfluidic Devices*, in *Microfluidics: Technologies and Applications*, B.C. Lin, Editor. 2011. p. 27-68.
- [4] Chen, H., et al., *High-throughput, deterministic single cell trapping and long-term clonal cell culture in microfluidic devices*. *Lab on a Chip*, 2014.
- [5] Chen, H.Y., et al., *Cardiac-like flow generator for long-term imaging of endothelial cell responses to circulatory pulsatile flow at microscale*. *Lab on a Chip*, 2013. **13**(15): p. 2999-3007.
- [6] Frenea-Robin, M., et al. *Contactless diamagnetic trapping of living cells onto a micromagnet array*. in *Engineering in Medicine and Biology Society, 2008. EMBS 2008. 30th Annual International Conference of the IEEE*. 2008.
- [7] Gassner, A.-L., et al., *Magnetic forces produced by rectangular permanent magnets in static microsystems*. *Lab on a Chip*, 2009. **9**(16): p. 2356-2363.
- [8] Gassner, A.L., et al., *Ring magnets for magnetic beads trapping in a capillary*. *Analytical Methods*, 2011. **3**(3): p. 614-621.
- [9] Gooneratne, C.P. and J. Kosel. *A micro-pillar array to trap magnetic beads in microfluidic systems*. in *Sensing Technology (ICST), 2012 Sixth International Conference on*. 2012.
- [10] Kim, C., et al., *Microfluidic chip for susceptibility of superparamagnetic nanoparticles of bead and droplet types and measuring method for susceptibility using the same*. 2013, Google Patents.
- [11] Nath, P., et al., *Rapid prototyping of robust and versatile microfluidic components using adhesive transfer tapes*. *Lab on a Chip*, 2010. **10**(17): p. 2286-2291.
- [12] Pamme, N., *Magnetism and microfluidics*. *Lab on a Chip*, 2006. **6**(1): p. 24-38.
- [13] Ramadan, Q., et al., *Magnetic-based microfluidic platform for biomolecular separation*. *Biomed Microdevices*, 2006. **8**(2): p. 151-8.
- [14] Schneider, C.A., W.S. Rasband, and K.W. Eliceiri, *NIH Image to ImageJ: 25 years of image analysis*. *Nat Meth*, 2012. **9**(7): p. 671-675.
- [15] Shevkoplyas, S.S., et al., *The force acting on a superparamagnetic bead due to an applied magnetic field*. *Lab on a Chip*, 2007. **7**(10): p. 1294-1302.
- [16] Shingi, H., et al., *Trapping and Collection of Lymphocytes Using Microspot Array Chip and Magnetic Beads*. *Japanese Journal of Applied Physics*, 2006. **45**(4R): p. 2850.
- [17] Tarn, M.D., S.A. Peyman, and N. Pamme, *Simultaneous trapping of magnetic and diamagnetic particle plugs for separations and bioassays*. *Rsc Advances*, 2013. **3**(20): p. 7209-7214.